On levitation by blowing

Paul K. Newton, and Y. Ma

Citation: American Journal of Physics **89**, 134 (2021); doi: 10.1119/10.0002032
View online: https://doi.org/10.1119/10.0002032
View Table of Contents: https://aapt.scitation.org/toc/ajp/89/2
Published by the American Association of Physics Teachers

On levitation by blowing

Paul K. Newton[a)]
Department of Aerospace and Mechanical Engineering, Mathematics, and Ellison Institute for Transformative Medicine, University of Southern California, Los Angeles, California 90089-1191

Y. Ma[b)]
Department of Physics and Astronomy, University of Southern California, Los Angeles, California 90089-1191

(Received 4 June 2020; accepted 9 September 2020)

Anyone who has visited a science museum has seen the demonstration where a beach (or ping-pong) ball is suspended in mid-air at a fixed position by constant blowing from below. After a while, the ball inevitably tumbles to the ground but can easily be rebalanced, by hand, again at the suspension point. Here, we ask a different more delicate question. Can we blow the ball from rest, starting at the nozzle opening ($x = 0$), moving it up to the suspension point $x = x^*$ above the nozzle? We show that it is not possible to do this using constant blowing because the point at which the downward gravitational force balances the upward blowing force is an elliptic fixed point of the governing equations, so there is no transfer trajectory that connects the origin to x^*. To overcome this problem, we design time-dependent blowing schedules that achieve the transfer, making use of orbit transfer ideas developed in the orbital mechanics literature. Then, we ask which of these time-dependent schedules are optimal? We show that, generally, it is bang–bang (on–off) blowing schedules that achieve the transfer in minimal time, using minimal energy (action) and minimal air volume. For certain parameter values, however, there are more complicated blowing schedules that are optimal (with respect to energy), which can be designed using the Pontryagin Maximum Principle (PMP) and singular control. We use elementary concepts from mechanics, nonlinear dynamics, and control theory and challenge the inclined experimentalist to try to implement some of these nonconstant blowing schedules in the lab.

https://doi.org/10.1119/10.0002032

I. INTRODUCTION

Is it possible to levitate a ping-pong ball from rest to a fixed height by constant blowing? At first glance, one might imagine that the answer is as simple as supplying a blowing force from below, which exactly balances the gravitational force pushing down at the height x^* where you want the ball to remain suspended, as shown in Fig. 1. An experiment, such as the one shown here (https://www.youtube.com/watch?v=bCRjPFhlSYk), might even confirm that it is achievable, as the ball is clearly suspended at the balance point x^*. Achieving this balancing act is not difficult, if one places the ball by hand at this point, and can be seen as a standard demonstration (typically using a beach ball) at science museums around the world. Here, we ask a different question. Instead of asking if a ball can be suspended at this point, we ask whether a ball, starting from rest at the base of the straw, $x = 0$, can be levitated to the point x^* using constant blowing. If one supplies a constant blowing force that is required to balance the ball at height $x^* > 0$, it turns out, surprisingly, that it is not possible to drive the ball from position $x = 0$ to position $x = x^*$ required for the forces to balance. We will show why and describe how to overcome the problem by using nonconstant blowing schedules designed appropriately. In short, we will show that the problem of balancing a ball at the fixed point $x = x^*$ using constant blowing is easier than blowing the ball from $x = 0$ to $x = x^*$ and having it remain there.

We formulate the problem as one in Hamiltonian mechanics, nonlinear dynamics, and optimal control theory and show how some blowing schedules are better than others. Some methods are borrowed from nonlinear orbit transfer ideas developed initially in the orbital mechanics literature[1] in which intersecting phase-space trajectories at different fixed parameter values are pieced together by switching from one parameter value to the other at precisely the time at which the trajectories intersect, creating a time-dependent control protocol that drives the system to a desirable state not achievable without the switching time. We became interested in developing these methods in the context of designing optimized time-dependent chemotherapy schedules in tumor growth models[2] that can steer the fitness landscape of the co-evolving cell populations in such a way as to delay chemotherapeutic resistance. While there is no connection between these models and the ones detailed in this paper, many of the mathematical techniques are quite similar. We develop the levitation problem from the ground up in terms that an undergraduate physics, engineering, or applied mathematics major could appreciate, and maybe in the process, learn some key ideas from control theory without the extra baggage of unnecessarily complex models and abstract mathematical notation.[3] Ideally, this article will stimulate readers to learn more about applications of control theory by reading the excellent article by Bechhoefer.[4]

Using air to levitate objects (as opposed to acoustic or magnetic levitation) is a common method of conveyance and has been explored in micro-manufacturing settings as discussed in Ref. 5, but to our knowledge, the observation that a nonconstant blowing is required to levitate an object to a fixed height has not been discussed in the literature. Reference 6 discusses the design of a low-cost air levitation system for teaching control engineering, and a more detailed recent description of a nice experimental setup that could be used to test the ideas in this paper is described in Ref. 7.

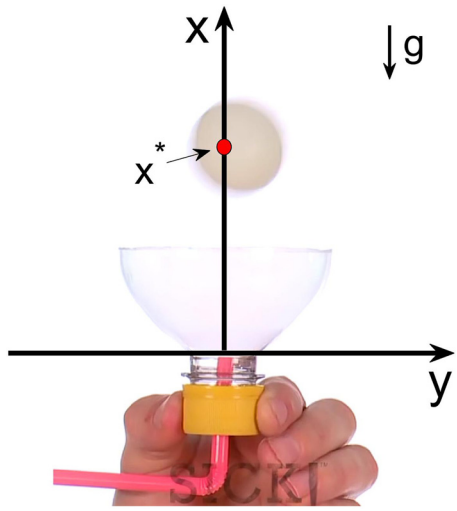

Fig. 1. Ping-pong ball suspended at a fixed height x^* by blowing through a straw. The streaming air blows upwards along the positive x direction against the gravity. x^* marks the equilibrium position where the forces balance, stabilized by the Bernoulli effect. Our question is not whether the ball can be suspended, as shown in the picture, but how we can drive (levitate) the ball from rest at $x=0$ to the equilibrium point $x=x^*$? For the full video, see https://www.youtube.com/watch?v=bCRjPFhlSYk.

II. THE MODEL

The model we consider is a simple dimensionless nonlinear system,

$$m\ddot{x} = -mg + mgb(t)\exp(-\alpha x). \tag{1}$$

Here, $b(t)$ is a dimensionless blowing parameter (proportional to the amount of air per unit of time) that we will use to levitate the ball from rest $v(0)=0$; $x(t)$ is the vertical height; m is the mass; and $\alpha>0$ is a constant that controls the distance over which the blower's influence is felt. (Our model is strictly one-dimensional because fluctuations from side to side are mollified by the Bernoulli effect as shown nicely in the following link: http://sciphile.org/lessons/bernoullis-beach-ball.) The ball starts at position $x(0)=0$ where the blower is located, as shown in Fig. 1, and the goal is to levitate it to height marked x^*. Our assumption in (1) is that the influence of the blowing decreases exponentially from the location of the blower ($x=0$), but our results are not sensitive to that choice, as long as the influence decreases monotonically with the height. We also assume that there is no frictional loss of energy as the ball levitates and that the ball does not rotate; hence, we treat it as a point mass. We emphasize that our model is simple in that it does not take into account the detailed fluid mechanical forces and dynamics at the jet-ball contact point (that would create effects such as dissipation and rotation of the ball). Our model is just complex enough to show that (i) it is not possible to drive the ball from its resting state at the base to the levitated state at height x^* with constant blowing and (ii) it is possible to drive the ball from its resting state to the levitated state by piecing together time-dependent blowing schedules with precise switching times determined from crossing phase-space trajectories. To levitate the ball initially, the upward blowing force must exceed the downward gravitational force at $x=0$, which implies that the right-hand side of Eq. (1) must be greater than zero (at $x=0$). The condition for this is that $b>1$.

The governing Hamiltonian for the system is given by

$$H(x,v) = \frac{1}{2}mv^2 + mgx + \frac{mgb\exp(-\alpha x)}{\alpha} \equiv E_b, \tag{2}$$

where we highlight the fact that b is a parameter, which we will vary in order to change energy values. Once b is fixed and the corresponding value E_b is chosen, Eq. (2) represents a curve (level curve) in the (x, v) plane. Notice that for fixed x and v, it is evident that $E_{b_1} > E_{b_2}$ when $b_1 > b_2$ since Eq. (2) is linear in b. The corresponding Hamiltonian equations of motion are

$$m\dot{x} = \frac{\partial H}{\partial v} = mv, \tag{3}$$

$$m\dot{v} = -\frac{\partial H}{\partial x} = -mg + mgb\exp(-\alpha x). \tag{4}$$

For any given b, the forces balance (i.e., acceleration is zero) when

$$x \equiv x^* = \frac{\ln(b)}{\alpha} \tag{5}$$

making the right-hand side of Eq. (4) zero. With the condition $b>1$, the equilibrium position is positive ($x^*>0$).

The phase-space diagram in the (x, v) plane, obtained from plotting level curves $H(x,v)=E_b=constant$, is shown in Fig. 2(a) for different energy values. The elliptic fixed point where the forces balance corresponds to

$$E_b^* = H(x^*,0) = \frac{mg}{\alpha}(\ln(b)+1). \tag{6}$$

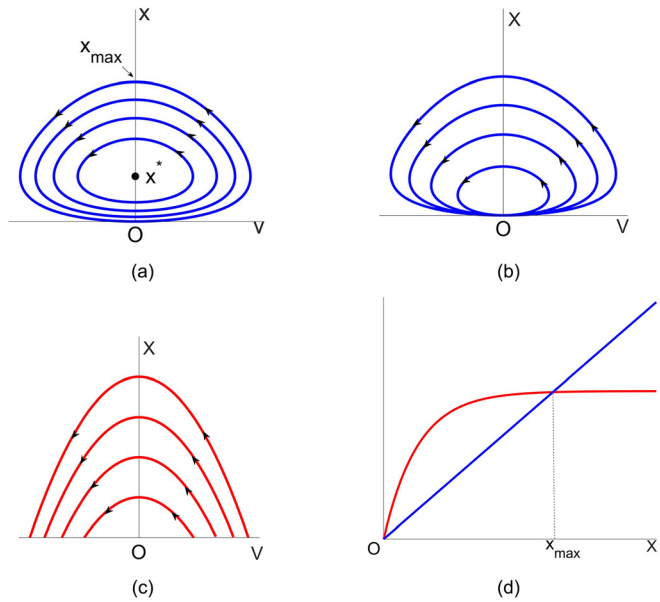

Fig. 2. (a) Phase curves in the (x, v) plane for five different values of the energy E_b. x_{max} marks the maximum height that the ball can achieve on the energy curve $E_b = E_b^0$, while the elliptic point x^* marks the levitation point where the forces balance $E_b = E_b^*$. (b) Energy curves $E_b = E_b^0$ going through the origin for four different values of b. (c) Phase curves of free fall ($b=0$) with different values of energy. (d) x_{max} marks the intersection of the two curves defined by the left (blue color online) and right (red color online) hand sides of Eq. (8).

At the origin where the blower is located, the energy value is

$$E_b^0 = H(0,0) = \frac{mgb}{\alpha} > E_b^*. \tag{7}$$

In Fig. 2(b), we show the curves E_b^0 for the increasing values of b. We also show in Fig. 2(c) the family of free-fall trajectories ($b=0$) associated with energy values $E_0 = \frac{1}{2}mv^2 + mgx$, which start at $(x, v) = (0, v^*)$.

To compute the point x_{max} shown in Fig. 2(a), we follow the phase curve that passes through the origin to the point x_{max}, using the fact that the Hamiltonian is constant, which gives rise to the transcendental equation for x_{max},

$$\alpha x_{\max} = b(1 - \exp(-\alpha x_{\max})). \tag{8}$$

The left and right sides of Eq. (8) are plotted in Fig. 2(d) where the intersection defines x_{max}. Because x^* is an elliptic fixed point, it is not possible to traverse from the origin to this point on a phase curve, i.e., there is no constant energy trajectory that passes both through the origin and x^*. Instead, the levitating ball starting at the origin will reach height $x_{\max} > x^*$ and then drop back down to the origin in a periodic orbit, always overshooting the height x^* where we want to position the ball.

For future use, notice that solving Eq. (2) for velocity yields

$$v = \pm\sqrt{\frac{2}{m}\left[E_b - mgx - \frac{mgb}{\alpha}\exp(-\alpha x)\right]}. \tag{9}$$

III. TIME-DEPENDENT BLOWING

To levitate the ball from the origin to x^*, we need to decrease the energy from its initial energy value E_b^0 to the final energy E_b^* by altering our blowing parameter b. Consider the family of phase curves for two different choices of the blowing parameter $b = b_1 > b_2 > 0$, as shown in Fig. 3. The diagram depicts two different paths to traverse from point O to point x^*. The blue (color online) curve corresponds to energy value $E_b = E_b^0$ for value $b = b_1$, giving rise to the elliptic balance point $x^*|_{b_1} = \ln(b_1)/\alpha$. The large dashed red (color online) curve that intersects $x^*|_{b_1}$ corresponds to energy value $E_b = E_b^0$ obtained by choosing blowing parameter $b = b_2 < b_1$, where $x_{\max}|_{b_2} = x^*|_{b_1}$. To traverse the dashed red (online) elliptical path that connects O to the resting point x^*, we first use blowing parameter value b_2, where $b_2 > 1$, until the ball arrives at x^*, say, at time $t = t_1$. Then, we can balance it there if we instantaneously change to the value $b_1 > b_2$ at t_1, which traps the ball at the elliptic fixed point. We call this a two-step schedule since it requires choosing two different values of b with one switch-time t_1. To calculate t_1, we evaluate $\int dx/v$ from O to x^* using Eq. (9),

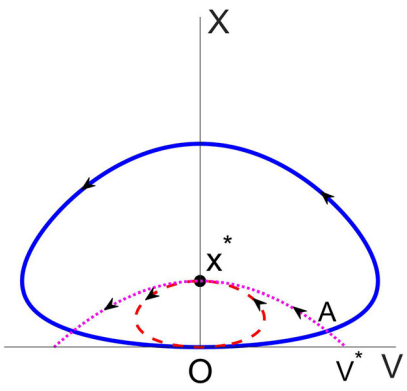

Fig. 3. Diagram showing two different paths from point O to point x^*. Orbits corresponding to energy $E_b = E_b^0$ for two different values, $b = b_1$ (blue online) and $b = b_2 < b_1$ (long dashed red online). Height x^* represents the elliptic fixed point associated with $b = b_1$. The value of b_2 is chosen so that x_{max} for the red (online) orbit intersects x^*. The small dashed pink (color online) orbit corresponds to a free-fall trajectory $b=0$ with an initial upward launch velocity v^* so that the trajectory intersects x^*. Point A, with coordinates (x_A, v_A), marks the intersection of the free-fall trajectory with the blue (color online) orbit.

$$t_1 = \int_0^{\ln(b_1)/\alpha} \frac{dx}{\sqrt{\frac{2}{m}\left[E_{b_2}^0 - mgx - \frac{mgb_2}{\alpha}\exp(-\alpha x)\right]}}. \tag{10}$$

A useful quantity to track is

$$S = \int_0^{t_f} E(t)dt, \tag{11}$$

which we think of as the action (since it has units of energy $\times$ time). If divided by the total time t_f over which it acts, it would be equivalent to the average energy expended. What is the value required to achieve a given transfer (t_f is the time the ball reaches x^*)? In this case, we have

$$S = E_{b_2}^0 \cdot t_1 \tag{12}$$

$$= \frac{mgb_2}{\alpha} \cdot t_1, \tag{13}$$

where $t_f \equiv t_1$. A second quantity we track is the area under the $b(t)$ curve,

$$B = \int_0^{t_f} b(t)dt, \tag{14}$$

which we think of as the total volume of air used to transfer the ball through time t_f. Similarly, if divided by the total time t_f through which it acts, it would be equivalent to the average value of the blowing parameter $b(t)$. In this case, we have

$$B = b_2 \cdot t_1. \tag{15}$$

The second path illustrated in Fig. 3, which takes the ball from O to x^*, traverses through point A. Consider the piecewise differentiable path $O \to A \to x^*$. On the first piece from $O \to A$, we launch the ball using blowing parameter value b_1 until time t_1 when we reach point A. At that time, we set $b=0$ and let the ball free-fall along path $A \to x^*$ on the small dashed pink curve (color online) until time t_2 when we arrive at x^*. This part of the path is described by the free-fall trajectory,

$$x = -\frac{1}{2}gt^2 + v_A t + x_A, \tag{16}$$

$$v = -gt + v_A, \tag{17}$$

where (x_A, v_A) marks the position and velocity coordinates at point A in Fig. 3. We know from Eq. (17) that $v = 0$ (maximum height) at time $t = v_A/g$. Therefore, for the total time to traverse the free-fall trajectory, we have

$$t_2 - t_1 = v_A/g. \tag{18}$$

Here, we use

$$t_1 = \int_0^{x_A} \frac{dx}{\sqrt{\frac{2}{m}\left[E^0_{b_1} - mgx - \frac{mgb_1}{\alpha}\exp(-\alpha x)\right]}}. \tag{19}$$

Eliminating t in Eqs. (16) and (17) gives the parabolic curve,

$$x = -\frac{v^2}{2g} + \left(\frac{v_A^2}{2g} + x_A\right), \tag{20}$$

beginning at (x_A, v_A) and ending at the point $(x^*, 0)$, where

$$x^* = \left(\frac{v_A^2}{2g} + x_A\right) = \frac{\ln(b_1)}{\alpha}. \tag{21}$$

At time t_2, we then let

$$b = b_1 = \exp\left[\alpha\left(\frac{v_A^2}{2g} + x_A\right)\right] \tag{22}$$

to trap the ball at this resting point. We call this a three-step sequence since it requires three sequential values of b $(b = b_1; b = 0; b = b_1)$ and two switching times t_1 and t_2. The total action along the trajectory is

$$S = E^0_{b_1} \cdot t_1 + E_0 \cdot (t_2 - t_1) \tag{23}$$

$$= \frac{mg}{\alpha}[b_1 \cdot t_1 + \ln(b_1)(t_2 - t_1)], \tag{24}$$

where E_0 is the free-fall value with $b = 0$, and $(x, v) = (x^*, 0)$, i.e., $E_0 = mgx*$. For this trajectory, we have

$$B = b_1 \cdot t_1 + 0 \cdot (t_2 - t_1) = b_1 \cdot t_1. \tag{25}$$

It is clear that once we allow for a time-dependent blowing function $b(t)$, there exist many schedules that allow us to achieve the goal of moving the ball from the origin to the resting point x^*, each taking a different total time to achieve the transfer and each requiring a different action value and air volume. We show in Table I numerically computed values for the two different paths described in Fig. 3, which shows the three-step path: $O \to A \to x^*$ (which includes a free-fall segment) is more efficient than the more direct two-step path: $O \to x^*$. A more comprehensive panel of schedules, using different fixed values of parameter b, and the trajectories that achieve the transfer to the levitation point, is shown in Fig. 4.

Table I. Time, action, and air volume values for two trajectories shown in Fig. 3. The results are simulated using the following variables: $b_1 = 6$, $\alpha = 1\ \mathrm{m}^{-1}$, $g = 9.8\ \mathrm{m/s}^2$, and $m = 1\ \mathrm{kg}$.

Path	Time t_f	Action S	Air volume B
$O \to x^*$	1.036	21.83	2.227
$O \to A \to x^*$	0.6662	16.84	0.7482

We are now in a position to formulate the problem as one in optimal control theory to ask, of all possible schedules, which one achieves the transfer from O to x^* in minimal time? Which transfer uses minimal action? Which transfer uses minimal amounts of air?

IV. OPTIMAL BLOWING SCHEDULES

Consider the problem of finding time-dependent blowing schedules $b(t)$ and the corresponding trajectories $(x(t), v(t))$ in the phase plane, which accomplish the task of moving the ball from (0, 0) to $(x^*, 0)$ in total time t_f, subject to the following equations:

$$m\ddot{x} = -mg + mgb(t)\exp(-\alpha x), \tag{26}$$

$$x(0) = 0; \dot{x}(0) = 0, \tag{27}$$

$$x(t_f) = x^*; \dot{x}(t_f) = 0. \tag{28}$$

We use the fact that $x \geq 0$, and we assume that the blowing function is bounded from below and above: $0 \leq b(t) \leq b_{\max}$.

A. Minimum time strategy

The transfer time t_f is given by

$$t_f = \int_0^{t_f} dt = \int_0^{x^*} \frac{dx}{dx/dt} = \int_0^{x^*} \frac{dx}{v}. \tag{29}$$

To minimize t_f, we need to minimize the area under $1/v(x)$ from $0 < x < x^*$, as shown in Eq. (29). We claim that a bang–bang strategy, in which we choose $b = b_{\max}$ initially, until switching time t_s at point $(x, v) = (x_s, v_s)$, when we choose a free-fall trajectory $b = 0$, accomplishes the minimization. To see this, consider the trajectories associated with the two extreme (constant) values $b = 0$ and $b = b_{\max}$ as shown in Fig. 5(a). The lower dashed red (online) trajectory is given by the curve using parameter value $E^0_{b_{\max}}$. At the switching time $t = t_s$, we switch the values of the blowing parameter to $b = 0$, so that the ball travels on a free-fall trajectory E_0 to the final resting point $(x^*, 0)$ at time t_f. These curves define a sector in the first quadrant of the (x, v) plane as shown in the figure. We show in Fig. 5(b) the same curves in the $1/v$ vs x plane and consider the areas under the curve using $E^0_{b_{\max}}$ from $0 < x < x_s$ and E_0 from $x_s < x < x^*$. In the interval $0 < x < x_s$, for any $(v(t), x(t))$ associated with the schedule $b(t)$, the following function will be used to derive the maximum velocity v_{max} for each fixed x,

$$\frac{d}{dt}\left(\frac{1}{2}v(t)^2 + gx(t) + \frac{b_{\max}g}{\alpha}e^{-\alpha x(t)}\right) \tag{30}$$

$$= (b(t) - b_{\max})vge^{-\alpha x(t)} \tag{31}$$

$$\leq 0. \tag{32}$$

Thus, the initial value gives the upper bound,

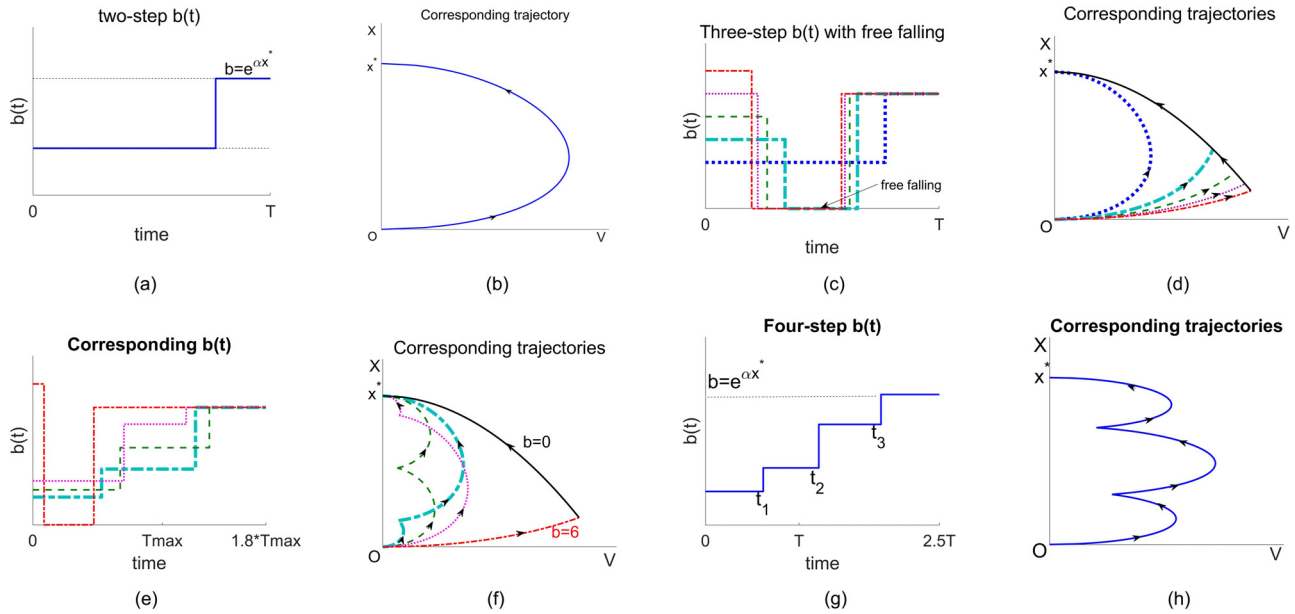

Fig. 4. Examples of piecewise constant blowing schedules that move the ball from the origin to the target point $(x, v) = (x^*, 0)$. Parameter values are given by $b \in [0, 6]$, $\alpha = 1\,\mathrm{m}^{-1}$, $g = 9.8\ \mathrm{m/s^2}$, $x^* = \ln(2)$ m, and $m = 1$ kg, and we choose $T = 1.34$ s for time scale. (a) Two-step schedule: $b(t)$ starts with $b = \alpha x^* e^{\alpha x^*}/e^{\alpha x^*} - 1$ and then switches to $b = e^{\alpha x^*}$. (b) The corresponding trajectories for the two-step schedule. Note that the ball will remain at equilibrium on second step, so the trajectory only has one segment. (c) Three-step schedule with blowing on the first segment, followed by free falling ($b = 0$) for the second segment. (d) The corresponding trajectory for (c). The trajectories will get closer and closer to the vertical axis with the increase in initial $b(t)$. (e) Examples of the general three-step schedule, with b_1 for the first segment and b_2 for the second. (f) The corresponding $b(t)$ for the examples of the general three step schedule. (g) A schematic of a four-step schedule where t_1, t_2, and t_3 mark three switching points. (h) The corresponding trajectory for (g).

$$\frac{1}{2}mv(t)^2 + mgx(t) + \frac{mb_{\max}g}{\alpha}e^{-\alpha x(t)} \tag{33}$$

$$\leq \frac{1}{2}mv(0)^2 + mgx(0) + \frac{mb_{\max}g}{\alpha}e^{-\alpha x(0)} \tag{34}$$

$$= \frac{mb_{\max}g}{\alpha} = E^0_{b_{\max}}. \tag{35}$$

From this, we know that $v(t)$ is bounded by

$$v \leq \sqrt{\frac{2}{m}\left[E^0_{b_{\max}} - gx - \frac{b_{\max}g}{\alpha}e^{-\alpha x}\right]} = v_{\max}. \tag{36}$$

Hence,

$$\int_0^{x_s}\frac{dx}{v_{\max}} < \int_0^{x_s}\frac{dx}{v}. \tag{37}$$

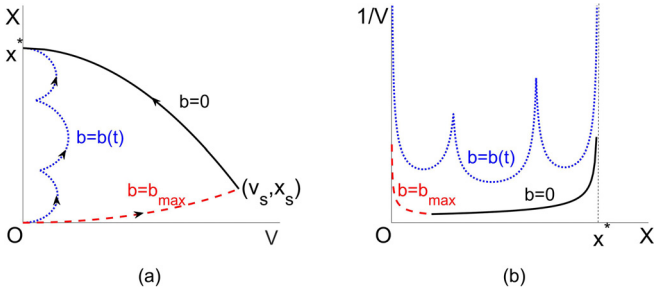

Fig. 5. (a) The schematic of the trajectory driven by a general blowing function $b(t)$ as indicated in blue (color online). For comparison, we show what we call the bang–bang strategy, starting with maximum blowing b_{max} from $t = 0$ to $t = t_s$ (dashed red online) and then free fall $b = 0$ from $t = t_s$ to $t = t_f$ (black). (b) Any trajectory associated with a more general blowing schedule $b(t)$ (solid blue online) lies above the lower two segments.

Similarly, in the interval $x_s < x < x^*$,

$$\frac{d}{dt}\left(\frac{1}{2}v(t)^2 + gx(t)\right) \tag{38}$$

$$= b(t)vg \tag{39}$$

$$\geq 0. \tag{40}$$

Thus, the final value gives the upper bound,

$$\frac{1}{2}v(t)^2 + gx(t) \tag{41}$$

$$\leq \frac{1}{2}v(t_f)^2 + gx(t_f) \tag{42}$$

$$= gx^*. \tag{43}$$

From this, we know that $v(t)$ is bounded by

$$v \leq \sqrt{2[gx^* - gx]} = v_{\max}. \tag{44}$$

Hence,

$$\int_{x_s}^{x^*}\frac{dx}{v_{\max}} < \int_{x_s}^{x^*}\frac{dx}{v}. \tag{45}$$

Therefore, the minimum-time transfer is achieved using the bang–bang strategy. An example of an optimal time trajectory and schedule is shown in Fig. 6.

B. Minimum air volume strategy

To minimize Eq. (14), first consider that

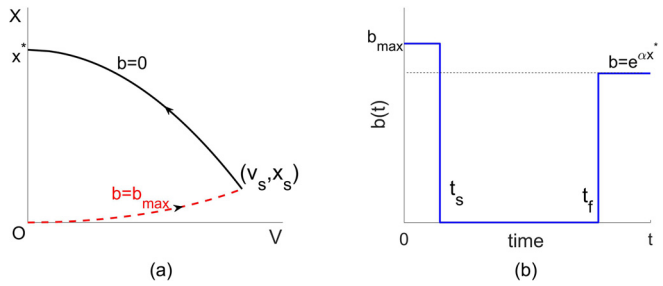

Fig. 6. The bang–bang (on–off) strategy is optimal to attain the transfer in minimum time and using minimum air volume. (a) The actual trajectory for the transfer. (b) The time-dependent blowing schedule that achieves the optimal transfer.

$$\dot{v} = \frac{dv(x)}{dx}\frac{dx}{dt} = v'(x)v \tag{46}$$

$$= -g + gb(t)\exp(-\alpha x), \tag{47}$$

which gives

$$b = \frac{v'(x)v + g}{g\exp(-\alpha x)}. \tag{48}$$

From this, we have

$$\int_0^{t_f} b(t)dt, \tag{49}$$

$$= \int_0^{x_f} b(t)\frac{dx}{v} \tag{50}$$

$$= \int_0^{x_f} \frac{v'(x)v + g}{g\exp(-\alpha x)}\frac{dx}{v} \tag{51}$$

$$= \int_0^{x_f} \frac{v'(x)}{g}\exp(\alpha x) + \int_0^{x_f} \frac{\exp(\alpha x)}{v}dx. \tag{52}$$

The first term can be integrated by parts, and using the fact that $v(0) = v(x_f) = 0$ gives

$$\int_0^{t_f} b(t)dt = \int_0^{x_f} \frac{\exp(\alpha x)}{v}dx - \int_0^{x_f} \frac{\alpha v}{g}\exp(\alpha x)dx. \tag{53}$$

It is easy to see that maximizing $v(x)$ will minimize both integrals, which gives the same result as the bang–bang strategy to minimize time (shown in Fig. 6).

C. Minimum action strategy

The problem of finding a minimum action strategy is more complicated. We start with

$$\int_0^{t_f} Hdt = \int_0^{t_f} (\frac{1}{2}v^2 + gx + \frac{bg\exp(-\alpha x)}{\alpha})dt \tag{54}$$

$$= \int_0^{t_f} \left(\frac{1}{2}v^2 + gx + \frac{\dot{v} + g}{\alpha}\right)dt \tag{55}$$

$$= \int_0^{x^*} \left(\frac{1}{2}v^2 + gx + \frac{\dot{v} + g}{\alpha}\right)\frac{dx}{v} \tag{56}$$

$$= \int_0^{x^*} \left(\frac{1}{2}v^2 + gx + \frac{\frac{dv}{dx}v + g}{\alpha}\right)\frac{dx}{v} \tag{57}$$

$$= \int_0^{x^*} \left(\frac{1}{2}v^2 + gx + \frac{g}{\alpha}\right)\frac{dx}{v} + \int_0^{x^*} \frac{dv}{\alpha}. \tag{58}$$

The last integral is simply $v(x^*) - v(0) = 0$, using the boundary conditions. So,

$$\int_0^{t_f} Hdt = \int_0^{x^*} f(v(x))dx, \tag{59}$$

$$f(v) = \left(\frac{1}{2}v^2 + gx + \frac{g}{\alpha}\right)\Big/ v. \tag{60}$$

To minimize this integral, we consider each fixed x and minimize with respect to $v(x)$, i.e.,

$$\frac{\partial f}{\partial v} = \frac{1}{2} - \frac{gx + \frac{g}{\alpha}}{v^2} = 0 \Rightarrow v(x) = \sqrt{2gx + \frac{2g}{\alpha}}. \tag{61}$$

However, the value above may not be achievable for all x, e.g., we have $v(x = 0) = 0$, so

$$v(x) = \begin{cases} \sqrt{2gx + 2g/\alpha}, & \sqrt{2gx + 2g/\alpha} \le v_{\max} \\ v_{\max}, & \sqrt{2gx + 2g/\alpha} \ge v_{\max}. \end{cases} \tag{62}$$

According to Fig. 7, if the switching point (v_s, x_s) is on the right side of the curve $v(x) = \sqrt{2gx + 2g/\alpha}$, then the extra transfer segment will exist connecting the b_{max} trajectory with the $b = 0$ trajectory. This gives a sufficient condition,

$$v_s > \sqrt{2gx_s + \frac{2g}{\alpha}}, \tag{63}$$

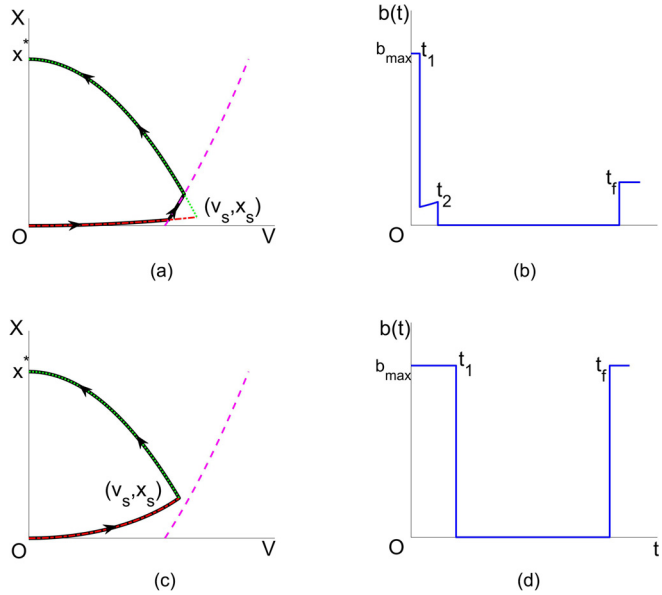

Fig. 7. Minimum action strategy. (a) Phase space trajectory using parameters $b_{max} = 20$, $\alpha = 1\,\mathrm{m}^{-1}$, $x^* = \ln(5)$ m, $g = 9.8$ m/s^2, and $m = 1$ kg. (b) Corresponding schedule for (a). (c) Phase space simulated with parameters: $b_{max} = 5$, $\alpha = 1\,\mathrm{m}^{-1}$, $x^* = \ln(5)$ m, $g = 9.8$ m/s^2, and $m = 1$ kg. (d) Corresponding bang–bang optimal control.

where

$$x_s = -\frac{\ln\left(1-\frac{\alpha x^*}{b_{\max}}\right)}{\alpha}, \tag{64}$$

$$v_s = \sqrt{2gx^* - 2gx_s}. \tag{65}$$

After we simplify the equations, we get

$$x_s < \frac{x^* - \frac{1}{\alpha}}{2}. \tag{66}$$

Meanwhile, the inequality is the necessary condition as well because the equations

$$x_s \geq \frac{x^* - \frac{1}{\alpha}}{2}, \tag{67}$$

$$v_{\max} \geq \sqrt{2gx + 2g/\alpha} \tag{68}$$

have no solution in the interval $0 < x < x_s$. In summary, Eq. (66) is both a necessary and a sufficient condition for the existence of the extra transfer segment shown in Fig. 7(a).

V. PONTRYAGIN MAXIMUM PRINCIPLE

The Pontryagin maximum (or minimum) principle (PMP)[8] is the most widely used method to find the optimal control scheme for certain dynamical systems. We will first give a statement of the PMP specifically for our problem. For proofs or more general versions, see Refs. 8–11.

Following the notation of Ref. 11, consider a general dynamical system with fixed initial condition $\mathbf{X}_0$, fixed final condition $\mathbf{X}_f$, and control $b(t)$,

$$\dot{\mathbf{X}}(t) = \mathbf{f}(\mathbf{X}(t), b(t)), \tag{69}$$

$$\mathbf{X}(0) = \mathbf{X}_0, \tag{70}$$

$$\mathbf{X}(t_f) = \mathbf{X}_f, \tag{71}$$

$$0 \leq b(t) \leq b_{\max}. \tag{72}$$

The goal is to minimize some objective function,

$$\min_{b(t)\in[0,b_{\max}]} \int_0^{t_f} L(\mathbf{X}(t), b(t))dt. \tag{73}$$

First, we construct the control theory Hamiltonian function $\mathbf{H}$ by introducing the Lagrange multiplier vector $\boldsymbol{\lambda}$,

$$\mathbf{H}\big(\mathbf{X}(t), \lambda(t), b(t)\big) = L + \boldsymbol{\lambda}^T\mathbf{f}. \tag{74}$$

The dynamical system for this optimal control problem is the same as Eqs. (3) and (4). We have

$$\mathbf{X} = (x(t), v(t))^T, \tag{75}$$

$$\mathbf{f} = (v(t), -g + gb(t)\exp(-\alpha x(t)))^T. \tag{76}$$

Suppose that $\boldsymbol{\lambda} = (\lambda_x, \lambda_v)^T$, and the control theory Hamiltonian function for this problem will be

$$\mathbf{H} = L + \lambda_x v + \lambda_v(-g + gb(t)\exp(-\alpha x)). \tag{77}$$

Assuming that $b^*(t)$ is our optimal control function, with the corresponding optimal trajectory $(x^*(t), v^*(t))$, there exist functions λ_x^*, λ_v^*, which satisfy the canonical equations of Hamilton,

$$\begin{aligned}
\dot{x}^* &= \frac{\partial \boldsymbol{H}(x^*, v^*, \lambda_x{}^*, \lambda_v{}^*, b^*)}{\partial \lambda_x}, \\
\dot{v}^* &= \frac{\partial \boldsymbol{H}(x^*, v^*, \lambda_x{}^*, \lambda_v{}^*, b^*)}{\partial \lambda_v}, \\
\dot{\lambda}^*{}_x &= -\frac{\partial \boldsymbol{H}(x^*, v^*, \lambda_x{}^*, \lambda_v{}^*, b^*)}{\partial x}, \\
\dot{\lambda}^*{}_v &= -\frac{\partial \boldsymbol{H}(x^*, v^*, \lambda_x{}^*, \lambda_v{}^*, b^*)}{\partial v}.
\end{aligned} \tag{78}$$

The optimal control $b^*(t)$ will minimize the control theory Hamiltonian $\mathbf{H}$ at any time point,

$$b^*(t) = \underset{b(t)\in[0,b_{\max}]}{\operatorname{argmin}} \mathbf{H}\big(x^*, v^*, \lambda_x^*, \lambda_v^*, b(t)\big). \tag{79}$$

If we leave the final time t_f as a free parameter, we need to impose one extra constraint on the final state,

$$\mathbf{H}\big(x^*(t_f), v^*(t_f), \lambda_x^*(t_f), \lambda_v^*(t_f), b^*(t_f)\big) = 0. \tag{80}$$

Together with the initial condition in Eq. (27) and the final condition in Eq. (28), the optimal control problem becomes a two-point boundary value problem. For the three cases, we considered in Sec. IV that $L = 1$ minimizes the time, $L = b(t)$ minimizes the air volume, and $L = H$ minimizes the average energy, respectively. It is not hard to observe that for all the cases, the control theory Hamiltonian $\mathbf{H}$ is linear with the control b, so Eq. (79) can be simplified based on the sign of $\partial\mathbf{H}/\partial b$,

$$b^*(t) = \begin{cases} 0, & \dfrac{\partial \boldsymbol{H}}{\partial b} > 0 \\ b_{\max}, & \dfrac{\partial \boldsymbol{H}}{\partial b} < 0. \end{cases} \tag{81}$$

This is the bang–bang schedule as calculated previously. The special case $\partial\mathbf{H}/\partial b = 0$ will be dealt with in Sec. V A. If $\partial\mathbf{H}/\partial b$ is nonzero almost everywhere, the optimal control $\mathbf{b}$ will be switching between 0 and b_{max} and thus a bang–bang control. After solving the two-point boundary value problem for $L = 1$ and $L = b(t)$, the optimal bang– bang control is identical to Sec. IV.

A. Singular control

For the minimum action case $L = H$, bang–bang control may not provide a solution to the two-point boundary value problem for the reason that $\frac{\partial \mathbf{H}}{\partial b} = 0$ will hold for at least some time interval, in which case the Pontryagin minimum principle fails to yield the complete solution. For this, we need to implement what is called singular control.[3]

The most simple method to solve this problem is to repeatedly differentiate $\partial\mathbf{H}/\partial b$ and set it to zero.[3,12] First, we know that

$$\frac{\partial \mathbf{H}}{\partial b} = 0 \tag{82}$$

for some time interval, so set the first order and second order time derivatives of $\partial \mathbf{H}/\partial b$ to 0 as well,

$$\frac{d}{dt}\left(\frac{\partial \mathbf{H}}{\partial b}\right) = 0, \tag{83}$$

$$\frac{d^2}{dt^2}\left(\frac{\partial \mathbf{H}}{\partial b}\right) = 0. \tag{84}$$

Since the canonical equations (78) give the formulas of $\dot{x}^*, \dot{v}^*, \dot{\lambda}_x^*, \dot{\lambda}_v^*$, the time derivatives can be easily calculated with the chain rule.

After solving Eqs. (82)–(84), we have the following:

$$\lambda_v^*(t) = -\frac{1}{\alpha}, \tag{85}$$

$$\lambda_x^*(t) = -v^*(t), \tag{86}$$

$$b^*(t) = 2e^{\alpha x^*(t)}. \tag{87}$$

Now, we achieve the formula for $b(t)$. We will show that Eq. (61) in Sec. IV (the transfer segment) is actually a singular arc. Take the time derivative of Eq. (61),

$$\begin{aligned}\frac{d}{dt}v(x) &= \frac{d}{dt}\sqrt{2gx + 2g/\alpha} \\ &= \frac{2g}{2\sqrt{2gx + 2g/\alpha}}\frac{dx}{dt} \\ &= \frac{g}{\sqrt{2gx + 2g/\alpha}}v \\ &= g.\end{aligned} \tag{88}$$

Together with Eq. (1), the control $b(t)$ for this segment will be

$$\begin{aligned}b(t) &= (\dot{v} + g)e^{\alpha x}/g \\ &= 2e^{\alpha x},\end{aligned} \tag{89}$$

which is identical to the singular arc in Eq. (87) [shown as the transfer segment in Fig. 7(a)].

VI. DISCUSSION

We have shown, using elementary classical mechanics, nonlinear dynamics, and control theory techniques, along with orbit transfer ideas,[1,2] that in almost all parameter cases, it is a bang–bang control schedule that achieves the transfer of the ball to the levitation point x^* in minimum time, with minimum air volume, while expending minimum action. There are, however, some parameter values for which a minimum action transfer is only achieved with the use of an extra transfer segment that connects two bang–bang arcs. The transfer formula is obtained analytically and is an example of the use of singular control methods,[3] which typically is not found in elementary texts on control theory. It might be of some interest to formulate similar optimal control problems associated with other forms of levitation, such as acoustic levitation or magnetic levitation with perhaps more complex models that include additional effects, such as dissipation, rotation, lateral stability/instability aspects, or even turbulent fluid fluctuations that might arise for small enough spheres (gas-fluidized levitating particles), as described in Ref. 13.

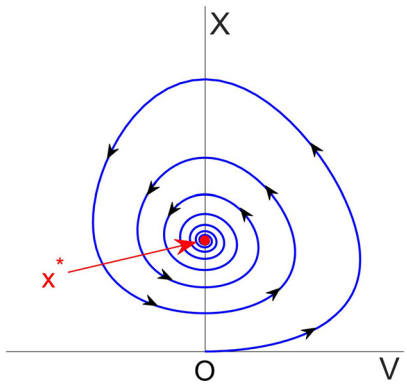

Fig. 8. Constant levitation with dissipation. The parameter values for the simulation are $b = 5$, $\alpha = 1\,\mathrm{m}^{-1}$, $g = 9.8\,\mathrm{m/s}^2$, $x^* = \ln(5)$ m, $m = 1$ kg, and $\gamma = 1$ kg/s.

It is also worth pointing out that aside from choosing an appropriate time-dependent function $b(t)$ to levitate the ball to the elliptic point, there are other physical mechanisms we could exploit. The simplest would be to add a small amount of dissipation to the model, proportional to the velocity,

$$m\ddot{x} = -mg + mgb(t)\exp(-\alpha x) - \gamma\dot{x}. \tag{90}$$

Here, γ is our dissipation parameter. In Fig. 8, we show a trajectory that ends up at x^* (as $t \to \infty$) after oscillating around it more and more tightly.

We end by posing a challenge to the experimentally inclined readers to design an experiment that makes use of the time-dependent schedules we describe in this paper. Will they accomplish the task, or are they perhaps unnecessary and need to be modified in light of the presence of dissipation in the system? Only a carefully designed experiment can sort this out.

ACKNOWLEDGMENTS

The problem arose while the authors were developing optimal control methods for time-dependent chemotherapy schedules that can outperform more traditional strategies when the authors realized there was a (mathematical) connection between the two problems. For this, the authors gratefully acknowledge partial support from the Breast Cancer Research Foundation (BCRF) and the Jayne Koskinas & Ted Giovanis Foundation (JKTG) for Health and Policy.

[a]Electronic mail: newton@usc.edu
[b]Electronic mail: yongqiam@usc.edu

[1]W. Koon, M. Lo, J. Marsden, and S. D. Ross, Chaos **10**, 427–469 (2000).
[2]P. Newton and Y. Ma, Phys. Rev. E **99**, 022404 (2019).
[3]A. E. Bryson, *Applied Optimal Control: Optimization, Estimation and Control* (Routledge, New York, 2018).
[4]J. Bechhoefer, Rev. Mod. Phys. **77**, 783–836 (2005).
[5]S. Konishi, M. Harada, Y. Ogami, Y. Daiho, Y. Mita, and H. Fujita, in IEEE 6th International Conference on Emerging Technologies and Factory Automation (1997), pp. 232–236.
[6]J. Chacon, J. Saenz, L. de la Torre, J. Diaz, and F. Esquembre, Sensors **17**, 2321–2339 (2017).

[7]A. Tootchi, S. Amirkhani, and A. Chaibakhsh, in Proceedings of 7th International Conference on Robotics and Mechatronics (ICRoM) (2019), pp. 29–34.
[8]L. S. Pontryagin, *Mathematical Theory of Optimal Processes* (CRC Press, Boca Raton, FL, 2018).
[9]E. B. Lee and L. Markus, *Foundations of Optimal Control Theory* (John Wiley and Sons, New York, 1967).
[10]I. Ross, *A Primer on Pontryagin's Principle in Optimal Control*, 2nd ed. (Collegiate Press, 2015).
[11]K. L. Teo, C. Goh, and K. Wong, "A unified computational approach to optimal control problems," (Pitman Monographs, New York, 1991).
[12]M. Zelikin and V. Borisov, J. Math. Sci. **130**, 4409–4570 (2005).
[13]R. Ojha, P. Lemieux, P. Dixon, A. Liu, and D. Durian, Nature **427**, 521–523 (2004).

Nörrenberg's Apparatus

The Nörrenberg doubler is a device for studying the effects produced by polarized light passing through thin transparent specimens. These might be naturally-occurring crystals, such as mica or Iceland spar, or two-dimensional crystals formed by the evaporation of solutions such as photographic hypo. Typically the specimen was placed on the mirror at the bottom so that the light passed through it in both directions. The eyepiece at the top contained a Nicol prism, a standard 19th century device for producing and analyzing polarized light. The initial polarized light was usually produced by reflecting a beam of unpolarized light from a plate of glass set at Brewster's angle. It was developed in 1858. This example is at Union College. (Picture and text by Thomas B. Greenslade, Jr., Kenyon College)